

Observed horizontal temperature advection by Tropical Instability Waves.

Markus Jochum, Meghan F. Cronin, William S. Kessler and Dennis Shea

submitted to GRL, 1/20/07

revised, 3/8/07

revised, 3/20/07

Corresponding author's address:

National Center for Atmospheric Research

1850, Table Mesa Drive

Boulder, CO, 80305

1-303-4971743

markus@ucar.edu

Abstract: Velocity data from moored current meters is combined with satellite sea surface temperature (SST) to compute oceanic mixed layer temperature advection by Tropical Instability Waves (TIWs). For the years 2002 to 2005 it is found that this process heats the equatorial mixed layer at an annual mean rate of + 0.8 °C/month at 0°N, 140°W and + 2.8 °C/month at 0°N, 110°W. At 0°N, 110°W, approximately 25 % of the heating is contributed by *zonal* temperature advection, a process that has often been assumed to be negligible. From a nine month segment of data (May 2004 - February 2005), the zonal temperature advection at 2°N, 140°W has been estimated to be approximately 0.7 °C/month, much larger than the equatorial value for the same time period. Thus, the data supports a recent hypothesis that tropical instability waves contribute a significant mean zonal temperature advection with off-equatorial maxima to the equatorial mixed-layer heat budget. Comparisons with numerical model results suggest that current ocean general circulation models can realistically simulate important aspects of tropical eddy-mixed layer interactions.

1 Introduction

TIWs are the result of instabilities of equatorial zonal currents (Philander 1976); their surface structure can be seen in satellite pictures of SST (e.g., Chelton et al., 2000; Figure 1) where they are observed in the eastern part of the Pacific basin between 4°S and 4°N as cusp-like features with wavelengths between 600 km and 2000 km and westward phase speeds between 20 cm/s and 60 cm/s. Hansen and Paul (1984) first discussed their importance for the equatorial mixed layer heat budget, and this topic is revisited here.

In numerical studies of the Atlantic (Jochum et al. 2005) and Pacific (Jochum and Murtugudde, 2006; JM hereafter) oceans it was shown that TIWs create strong vertical entrainment events that mix heat from the surface into the thermocline. This is because TIWs, whether they are waves or vortices, lift and depress the thermocline and mixed layer. Because they are not geostrophically balanced, there will be a zonal convergence into the centers of the TIW cyclones where the shoaling of the mixed layer causes strong entrainment (JM). Since this cools SST, the ocean latent and sensible heat loss is reduced which leads to a net ocean heat uptake.

The mechanism that gives rise to zonal temperature advection relies on the fact that part of TIW energy is projected onto first meridional mode Rossby waves (Cox 1980). These waves consist of alternating cyclones and anticyclones just to the north and south of the equator (Matsuno 1966), which are not in geostrophic balance close to the equator. Thus, the cyclones are associated both with thermocline uplift (which thins the mixed layer and enhances vertical mixing), and

near-surface convergence. This combination produces a large advective warming in the mixed layer as warm water from the edges encounters the shallow isotherms. It will be shown that the magnitude of this off-equatorial heating can be as large as that due to the widely-appreciated meridional temperature advection on the equator.

The efficiency of this TIW heat pump depends on the phase relationship between mixed layer depth variations, SST and zonal velocities. JM showed that the efficiency is maximal for first meridional mode Rossby waves. Thus, zonal temperature advection of TIWs will critically depend on how the energy of the instabilities is projected onto the different wave modes. This could be highly model dependent, so it is reassuring that the modelling studies of Kessler et al. (1998), who, like JM, use a sigma-layer model with a bulk mixed layer, and Menkes et al. (2006), who use a z-level model with parameterized vertical mixing, both report significant zonal temperature advection by TIWs too. Moreover, the results of the 2.5 layer model of McCreary and Yu (1992) are also consistent with strong off-equatorial zonal temperature advection. Nevertheless, this concept of how TIWs interact with the mixed layer is new and based largely on model results; therefore it needs observational verification which is the focus of the present study.

Since the mean zonal SST gradient is near-zero, zonal temperature advection is dependent on the mesoscale zonal SST gradient created by TIWs, and on vertical mixing (for the sake of simplicity we assume that the mixed layer temperature is identical to SST). JM estimate that in their model approximately 50% of the

equatorial (New Guinea to South America, 4°S to 4°N) atmosphere-ocean heat flux enters the thermocline through TIWs, much of it via zonal temperature advection at 2°N (Figure 2) where the TIW induced zonal SST gradient is largest (Liu et al. 2000). In classical treatments of TIW heat flux (Hansen and Paul, 1984; Bryden and Brady, 1989; Baturin and Niiler, 1997) the data was insufficient to measure zonal temperature advection, although mesoscale zonal SST gradients can be as large as meridional SST gradients (Liu et al. 2000). To our knowledge there are no direct observations of this process, although some observational support for its existence comes from the analysis of drifter data in the TIW Experiment (Kennan and Flament, 2000), and from the analysis of velocity and density gradients across the equatorial SST front (Johnson, 1996).

Previous studies combining satellite-based SSTs with moored current meter data could not adequately address the issue of eddy fluxes, because the spatial and temporal resolution of the available SST data was insufficient to compute SST gradients on TIW scales (Wang and McPhaden, 2001; Wang and Weisberg, 2001). Two advances are fundamental to the present study: A new theory that motivates revisiting TIW fluxes (JM), and new, high resolution SST observations (Tropical Rainfall Measuring Mission (TRMM) Microwave Imager (TMI)).

Here, estimates are presented for TIW temperature advection in the mixed layer on the equator at 140°W and 110°W, and at 2°N, 140°W. The estimates are based on mooring and satellite observations and are consistent with the theory and model-based expectations of JM.

2 Data and Results

Velocity data used here are from Sontek Argonaut single-point, acoustic doppler current meters mounted at 10 m depth on three moorings: the 0°N , 110°W and 0°N , 140°W Tropical Atmosphere Ocean (TAO) moorings, and a temporary Pacific Marine Environmental Laboratory (PMEL) engineering development mooring next to the standard 2°N , 140°W TAO mooring. In the absence of a high density mooring array the analysis had to be restricted to the mixed layer where the SST gradient is available in high resolution (0.25°) through the TMI of the TRMM (Gentemann et al. 2004; data available from www.ssmi.com). During the TRMM mission in the TIW domain, only the two equatorial current meters provide velocities in the mixed layer for a time sufficiently long to arrive at statistically significant results. However, since theory predicts an off-equatorial maximum of zonal eddy temperature advection (JM), it seems worthwhile to include the nine month data set from 2°N , 140°W in the analysis as well. Although nine months is too short to subject this data to statistical tests, it is studied here because it bears importantly on the spatial structure of the eddy heating, which is an important part of the theory.

At the three mooring locations the TMI data can be checked against *insitu* temperature (Figure 3): the correlation, based on daily averaged data, between the satellite data and mooring temperature at 10m is 0.91 (0°N , 110°W), 0.96 (0°N , 140°W), and 0.93 (2°N , 140°W , 20m), with the mean mooring temperature

being 0.29C, 0.23C, and 0.19C warmer, respectively. Since the bias is similar for all moorings, we assume that the following results, which only rely on the SST gradient, will not be changed substantially by a bias in the SST data.

At the equatorial locations the mean horizontal temperature advection (uT_x, vT_y) is small compared to the TIW induced temperature advection and not statistically different from zero (not shown). In JM's model, too, mean temperature advection is relatively small and not significantly different from zero. In model and observations, the relatively small mean temperature advection can be explained by both large intraseasonal variability and strong seasonally reversing currents on top of a weak mean flow. For the off-equatorial site the time series is too short to determine the annual mean and its interannual variations. TIWs, however, are plentiful and it is possible to derive meaningful estimates for the eddy temperature advection.

For each location the eddy zonal and meridional temperature advection were computed as respectively $u'T'_x$ and $v'T'_y$, where the prime indicates the TIW part of the spectrum. This has been computed by removing the atmospherically induced 3-5 day variability (Jones et al., 1998) from the time series with a 7-day Hanning smoother, and by removing the longer periods with a 51 day Hanning smoother. 51 days is longer than the TIW period of 15-40 days (Lyman et al., 2006) and going to a 61 or 71 day Hanning smoother changes the following results by less than 5%.

In all records the intraseasonal variability caused by TIWs is clearly visible

(see Figure 3 as an example). Gaps in data coverage which occur occasionally in the current meter record do not enter the calculations, so no interpolation has been done. Thus, the results at 0°N , 110°W are based on 668 days of data, the results at 0°N , 140°W are based on 1038 days, and the results at 2°N , 140°W on 281 days. Computing the annual mean eddy temperature advection is then straightforward. In Tables 1-3 the overbar denotes the mean over the record length, and the standard deviation is based on the means of 4 (Table 1) and 6 (Table 3) individual years. Using the *Student's - t* distribution yields an 80% confidence level for the values in Tables 1 and 3. For the short time series at 2°N , 140°W the standard deviation could not be computed meaningfully. For orientation, note that negative values indicate warming and that for a 30 m deep mixed layer a heating rate of $2^{\circ}\text{C}/\text{month}$ is equivalent to a heat flux convergence of $93 \text{ W}/\text{m}^2$. The observations (Tables 1 and 2) are consistent with JM's model results (based on 6 years, forced with climatological winds) shown in Table 3.

Apart from the overall agreement between model and observations, it is the main result of the present study that, as predicted in JM, there is a net rectified zonal temperature advection caused by TIWs (0°N , 110°W ; 2°N , 140°W), and that its maximum is off the equator: at 140°W ; for the covered time, TIW induced warming of the mixed layer at the equator is $0.08^{\circ}\text{C}/\text{month}$, whereas at 2°N it is $0.68^{\circ}\text{C}/\text{month}$.

Since the time series at 2°N is rather short it is worthwhile taking a closer look at the data and check whether it is consistent with the process for zonal,

off-equatorial eddy temperature advection described in JM. Because TIWs are not geostrophically balanced, there is a zonal convergence into the centers of the TIW cyclones where the shallowing of the mixed layer causes strong entrainment. Thus, eastward as well as westward flow creates heating. This is indeed seen in the data (Figure 4, top): the three largest events show a reversal of flow in August/September and November/December, and the heating maxima occur when the flow is strongest, independent of its direction. Thus, the center of a cyclone (and the mixing) is supplied by warm water from the east *and* the west, and since mixing is an irreversible process there is net heating. This mechanism is strongest for a first meridional mode Rossby wave (JM) which implies a phase lag between zonal velocity and SST of 90° . A lag correlation analysis for SST and zonal velocity (Figure 4, bottom) produces a maximum correlation of 0.53 for a lag of 8 days. For a 32-day wave period (within the expected TIW period range of 15-40 days) this is consistent with the theoretically predicted quarter wave period phasing.

3 Summary and Discussion

Satellite based SST observations have been combined with moored velocity data to compute the temperature advection of TIWs in three equatorial locations. For the years 2002 to 2005 it is found that this process heats the equatorial mixed layer at an annual mean rate of $+ 0.8^\circ\text{C}/\text{month}$ at 140°W and $+ 2.8^\circ\text{C}/\text{month}$ at 110°W . At 110°W , approximately 25 % of the heating is contributed by *zonal* temperature advection. From a nine month segment of data (May 2004 - February 2005), the heating due to zonal temperature advection at 2°N , 140°W has been estimated to be approximately $+ 0.7^\circ\text{C}/\text{month}$, much larger than the equatorial value for the

same time period.

The results support the hypothesis put forward in JM: Zonal temperature advection by TIWs is as important as their meridional temperature advection, and is therefore a significant contributor to the mixed layer heat budget. This implies that previous studies on the equatorial mixed layer heat budget (e.g.; Wang and McPhaden 1999) lack an important heating term and are likely to underestimate the vertical entrainment along the equator which is usually determined as a residual.

TIW temperature advection as evaluated here is an abstract number which by itself does not reveal the underlying process. Therefore, the present study is merely a starting point from which one should set out trying to understand eddy induced entrainment. The present study gives evidence to support the hypothesis that TIWs significantly increase the air-sea heat flux (JM), and can therefore contribute to interannual SST variability (Jochum and Murtugudde 2004). Although the zonal temperature advection quantified here is a key piece of evidence, the connection between temperature advection and air-sea heat flux has not been demonstrated here. To establish and quantify this connection it is necessary to obtain high resolution observations of surface fluxes (available from TAO buoys, Cronin et al. 2006), and of mixed layer depth, which is currently not available for all the discussed sites and times. Regarding the physical mechanism, a still unanswered question is what exactly is responsible for increased entrainment in TIW cyclones. It could be that more turbulent kinetic wind energy is available to

penetrate beneath the mixed layer, it could be increased vertical current shear, or both. In the first case the surface wind will be of paramount importance in determining the TIW induced air-sea heat flux. Given the magnitude of the TIW induced off-equatorial heating, the details of the TIW induced heating will place a new, severe constraint on the air-sea heat fluxes in coupled climate models, most of which do not resolve TIWs.

Acknowledgements: MJ and DS are funded through NCAR by NSF. MFC and WSK are funded through PMEL by NOAA. The mooring data is provided by PMEL (<http://www.pmel.noaa.gov/tao>) and the satellite data by the TRMM project through Remote Sensing Systems. We thank Peter Gent and Bill Large for insightful discussions. This study has been done as part of a NASA grant that supports the determination of eddy fluxes through space based instruments. This publication is PMEL contribution 3018.

References

- Baturin, N., Niiler, P., 1997. Effects of instability waves in the mixed layer of the equatorial Pacific. *J.Geophys.Res.* 102, 27771–27793.
- Bryden, H., Brady, E., 1989. Eddy momentum and heat fluxes and their effects on the circulation of the equatorial Pacific ocean. *J.Mar.Res.* 47, 55–79.
- Chelton, D. B., Wentz, F. J., Gentemann, C. L., de Szoeke, R. A., Schlax, M. G., 2000. Satellite microwave SST observations of transequatorial tropical instability waves. *Geophys. Res. Lett.* 27, 1239–1242.
- Cox, M., 1980. Generation and propagation of 30-day waves in a numerical model of the Pacific. *J.Phys.Oceanogr.* 10, 1168–1186.
- Cronin, M. F., Fairall, C. W., McPhaden, M. J., 2006. An assessment of buoy-derived and numerical weather prediction surface heat fluxes in the tropical Pacific. *J. Geophys. Res.* 111, doi:10.1029/2005JC003324.
- Gentemann, C., Wentz, F., Mears, C., Smith, D., 2004. In situ validation of Tropical Rainfall Measuring Mission microwave sea surface temperatures. *J. Geophys. Res.* 109, doi:10.1029/2003JC002092.
- Hansen, D., Paul, C., 1984. Genesis and effects of long waves in the equatorial Pacific. *J.Geophys.Res.* 89, 10431–10440.
- Jochum, M., Murtugudde, R., 2004. Internal variability in the tropical Pacific ocean. *Geophys. Res. Lett.* 31, L14309, doi:10.1029/2004GL020488.
- Jochum, M., Murtugudde, R., 2006. Temperature advection by Tropical Instability Waves. *J. Phys. Oceanogr.* 36, 592–605.

- Jochum, M., Murtugudde, R., Ferrari, R., Malanotte-Rizzoli, P., 2005. The impact of horizontal resolution on the equatorial mixed layer heat budget in ocean general circulation models. *J. Climate* 18, 841–851.
- Johnson, E. S., 1996. A convergent wave front in the central tropical Pacific. *Deep-Sea Res. II* 43, 753–778.
- Jones, C., Waliser, D. E., Gautier, C., 1998. The Influence of the Madden-Julian Oscillation on Ocean Surface Heat Fluxes and Sea Surface Temperature. *J. Clim.* 11, 1057–1072.
- Kennan, S. C., Flament, P. J., 2000. Observations of a tropical instability vortex. *J. Phys. Oceanogr.* 30, 2277–2301.
- Kessler, W. S., Rothstein, L. M., Chen, D., 1998. The annual cycle of SST in the eastern tropical Pacific as diagnosed in an OGCM. *J. Clim.* 11, 777–799.
- Liu, W. T., Xie, X., Polito, P. S., Xie, S. P., Hashizume, H., 2000. Atmospheric manifestation of TIWs observed by QuikSCAT and TRMM. *Geophys. Res. Lett.* 27, 2545–2548.
- Lyman, J. M., Johnson, G. C., Kessler, W. S., 2005. Separate 20-day and 30-day Tropical Instability Waves in subsurface temperature observations. submitted to *J. Phys. Oceanogr.* .
- Matsuno, T., 1966. Quasi-geostrophic motions in equatorial areas. *J. Meteorol. Soc. Jpn.* 2, 25–43.
- McCreary, J. P., Yu, Z., 1992. Equatorial dynamics in a 2.5-layer model. *Prog. Oceanogr.* 29, 61–132.

- Menkes, C. E. R., Vialard, J. G., Kennan, S. C., Boulanger, J.-P., Madec, G. V., 2006. A modelling study of the impact of tropical instability waves on the heat budget of the eastern equatorial Pacific. *J. Phys. Oceanogr.* 36, 847–865.
- Philander, S., 1976. Instabilities of zonal equatorial currents - Part 1. *J. Geophys. Res.* 81, 3725–3735.
- Wang, C., Weisberg, R. H., 2001. Ocean circulation influences on sea surface temperature in the equatorial central Pacific. *J. Geophys. Res.* 106, 19515–19526.
- Wang, W., McPhaden, M. J., 1999. The surface-layer heat balance in the equatorial Pacific ocean. Part I: mean seasonal cycle. *J. Phys. Oceanogr.* 29, 1812–1831.
- Wang, W., McPhaden, M. J., 2001. The surface-layer temperature balance in the equatorial Pacific during the 1997-98 El Nino and 1998-99 La Nina. *J. Clim.* 14, 3393–3407.

Figure 1: SST on August 29, 2004, from TRMM satellite. TIWs can be identified as the wave pattern along the equator with approximately 1000 km wavelength. The boxes indicate the location of the sites analyzed in the text.

Figure 2: Temperature advection by TIW at 140°W (top) and 110°W (bottom) predicted from JM. Solid line is meridional advection, broken line is zonal advection. Note that the zonal temperature advection is not compensated for by cooling further east or west (JM).

Figure 3: Zonal velocity at 10m depth from the mooring at 2°N , 140°W (top); temperature from SSMI (solid line) and at 20 m depth from the TAO mooring (broken line) at 2°N , 140°W (bottom).

Figure 4: Band-pass filtered Zonal velocity (broken line) at 10m depth from the mooring at 2°N , 140°W , and zonal eddy temperature advection (top). Bottom: Band-passed filtered zonal velocity (broken line, like above) and SST 2°N , 140°W .

position	term	observed value [$^{\circ}\text{C}/\text{month}$]
0 $^{\circ}$ N, 110 $^{\circ}$ W	$\overline{u'T'_x}$	-0.69 ± 0.47
	$\overline{v'T'_y}$	-2.09 ± 0.89
0 $^{\circ}$ N, 140 $^{\circ}$ W	$\overline{u'T'_x}$	$+0.07 \pm 0.30$
	$\overline{v'T'_y}$	-0.82 ± 0.41

Table 1: Observed mean TIW temperature advection along the equator.

position	term	observed value [$^{\circ}\text{C}/\text{month}$]
0 $^{\circ}$ N, 140 $^{\circ}$ W	$\overline{u'T'_x}$	-0.08
	$\overline{v'T'_y}$	-0.91
2 $^{\circ}$ N, 140 $^{\circ}$ W	$\overline{u'T'_x}$	-0.68
	$\overline{v'T'_y}$	-0.22

Table 2: Observed mean TIW temperature advection along 140 $^{\circ}$ W for the concurrent period of 9 months.

position	term	modelled value [$^{\circ}\text{C}/\text{month}$]
0 $^{\circ}$ N, 110 $^{\circ}$ W	$\overline{u'T'_x}$	-0.85 ± 0.23
	$\overline{v'T'_y}$	-3.04 ± 0.58
0 $^{\circ}$ N, 140 $^{\circ}$ W	$\overline{u'T'_x}$	-0.17 ± 0.10
	$\overline{v'T'_y}$	-1.40 ± 0.29
2 $^{\circ}$ N, 140 $^{\circ}$ W	$\overline{u'T'_x}$	-0.88 ± 0.24
	$\overline{v'T'_y}$	$+0.22 \pm 0.43$

Table 3: Modelled mean TIW temperature advection along 140 $^{\circ}$ W and along the equator.

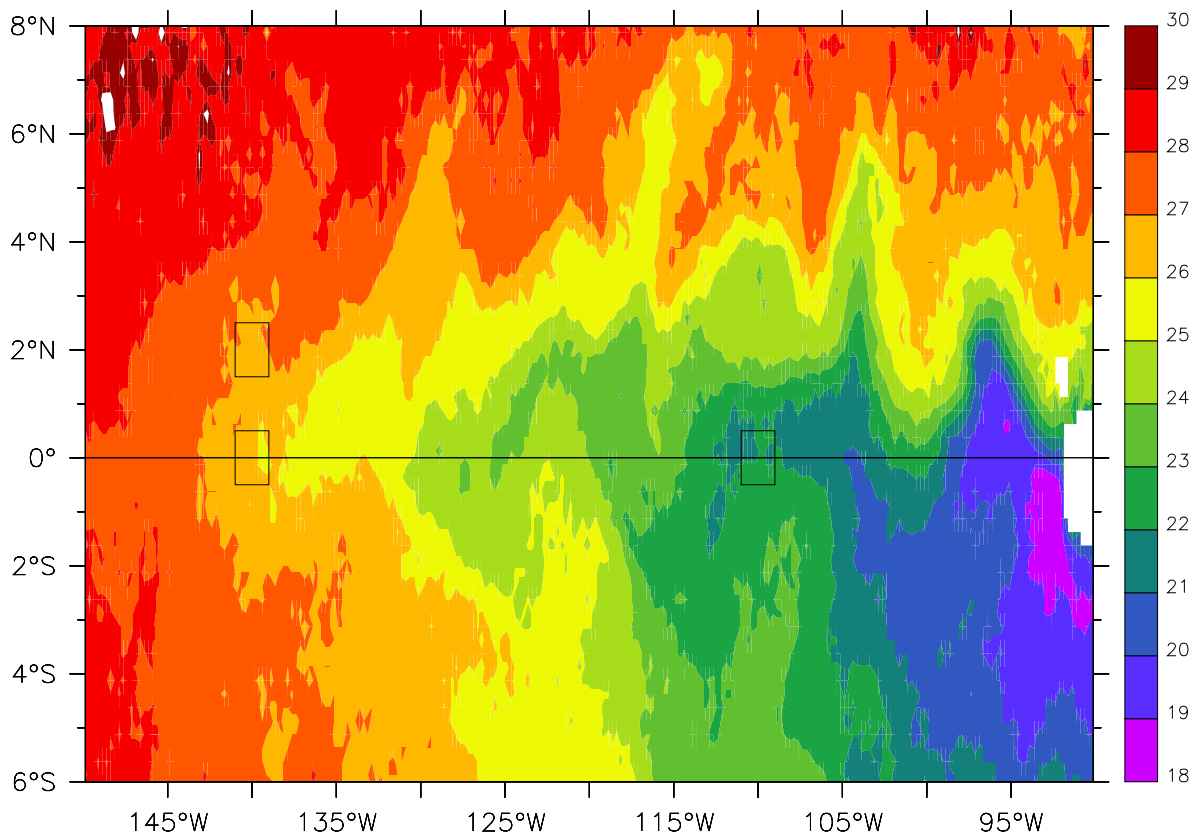


Figure 1: SST on August 29, 2004, from TRMM satellite. TIWs can be identified as the wave pattern along the equator with approximately 1000 km wavelength. The boxes indicate the location of the sites analyzed in the text.

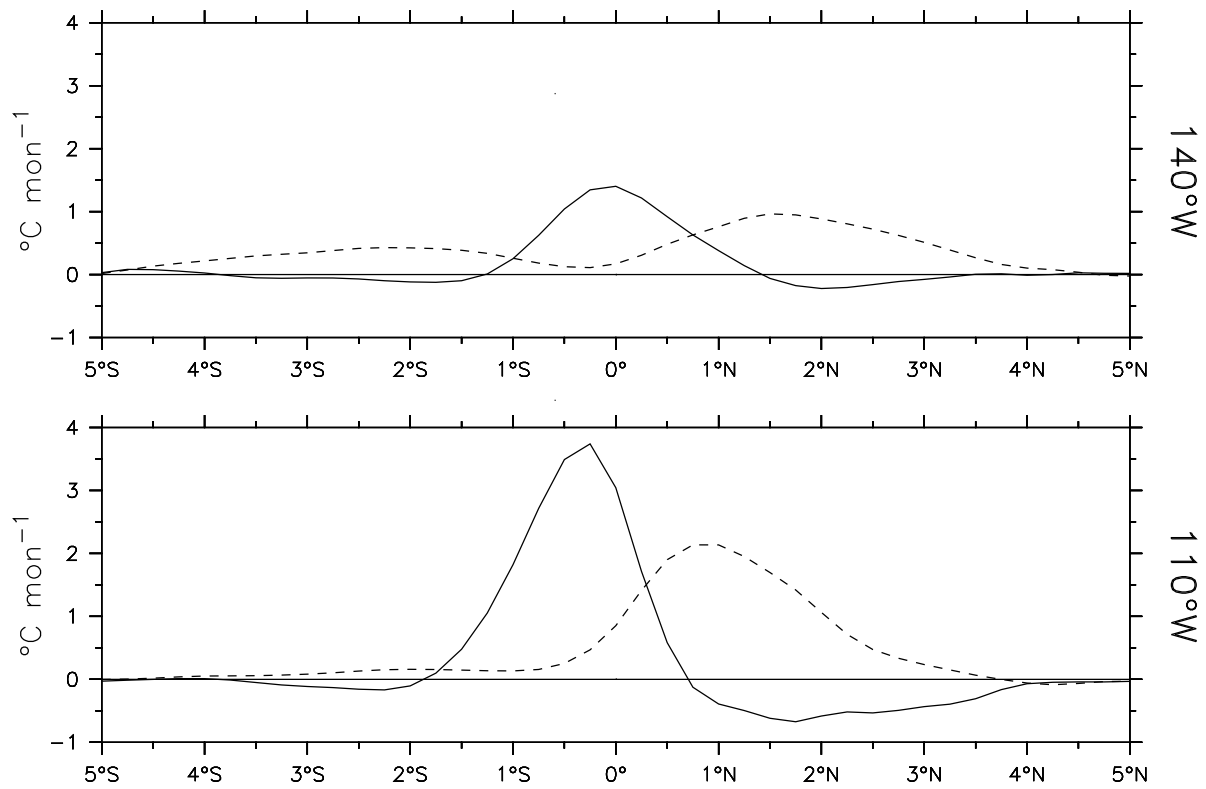


Figure 2: Temperature advection by TIW at 140°W (top) and 110°W (bottom) predicted from JM. Solid line is meridional advection, broken line is zonal advection. Note that the zonal temperature advection is not compensated for by cooling further east or west (JM).

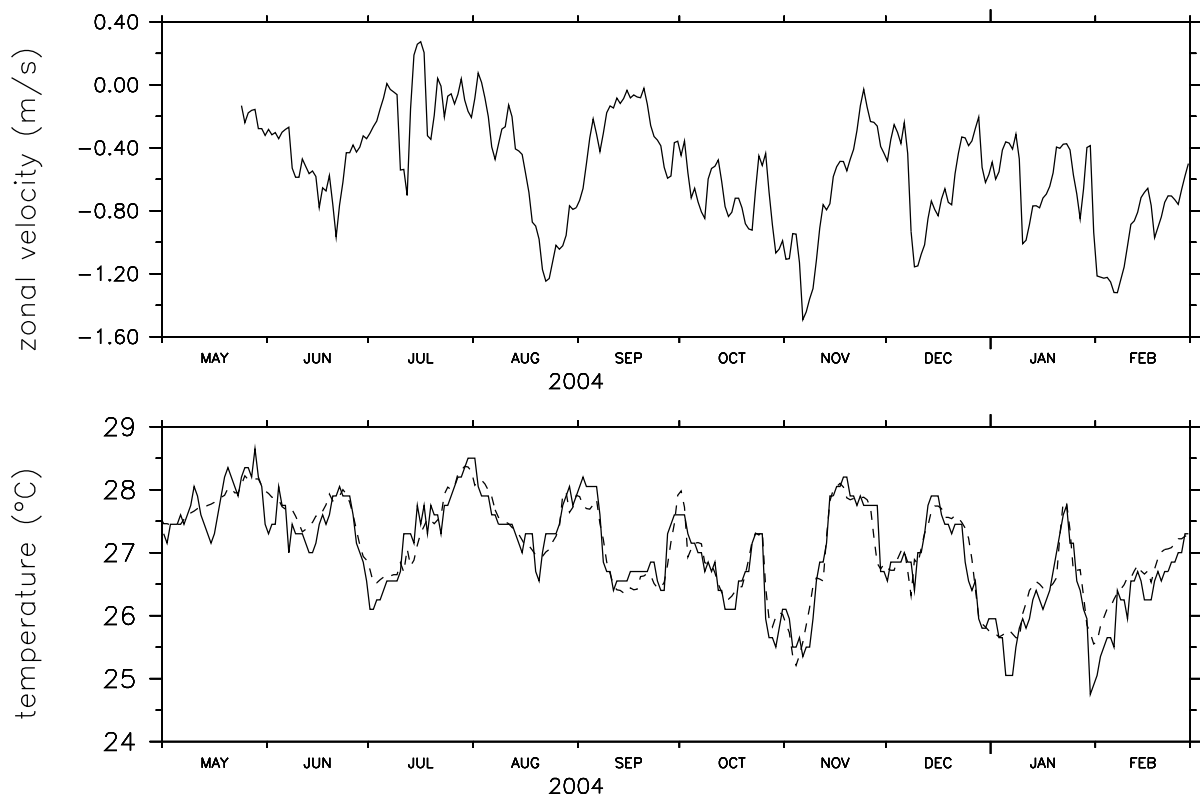


Figure 3: Zonal velocity at 10m depth from the mooring at 2°N, 140°W (top); temperature from SSMI (solid line) and at 20 m depth from the TAO mooring (broken line) at 2°N, 140°W (bottom).

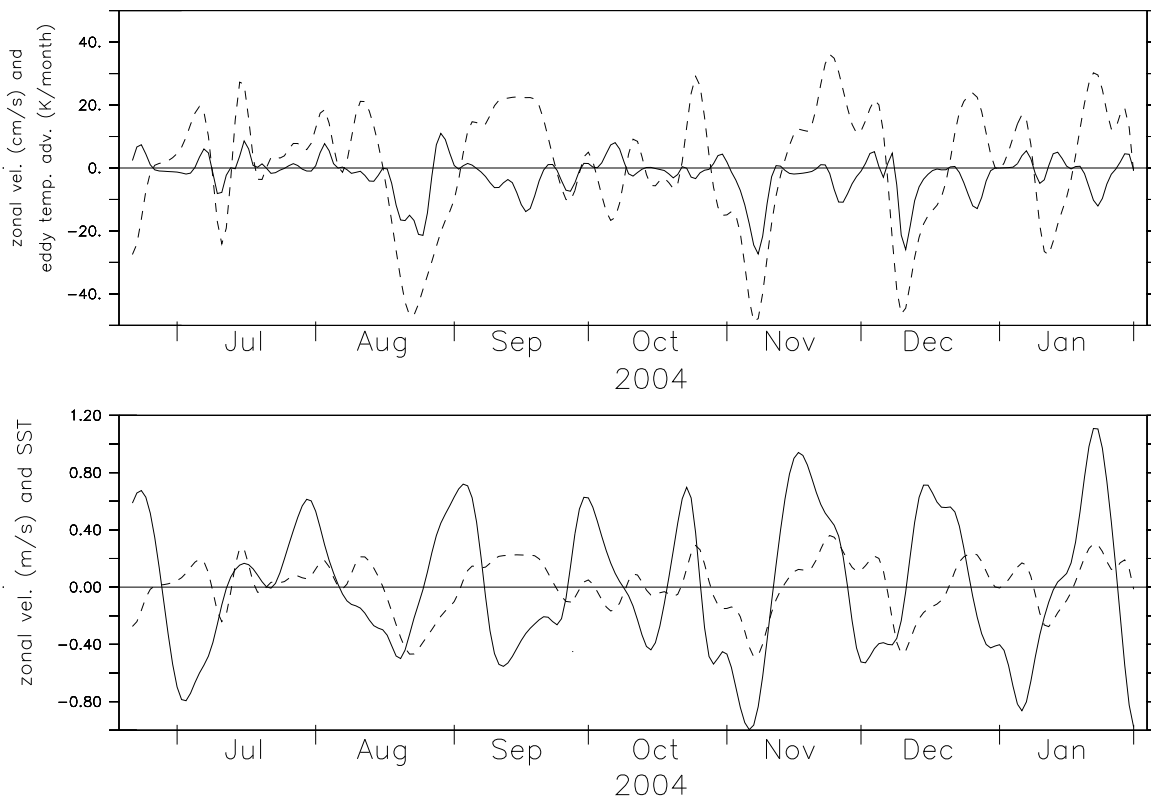


Figure 4: Top: Band-pass filtered zonal velocity (broken line) at 10m depth from the mooring at 2°N, 140°W and zonal eddy temperature advection. Bottom: Band-pass filtered zonal velocity (broken line, like above) and SST at 2°N, 140°W.